doi:10.1111/j.1365-2591.2006.01143.x

Cyclic fatigue resistance and three-dimensional analysis of instruments from two nickel–titanium rotary systems

N. M. Grande[1], G. Plotino[1], R. Pecci[2], R. Bedini[2], V. A. Malagnino[3] & F. Somma[1]

[1]Department of Endodontics, Catholic University of Sacred Heart; [2]Technology and Health Department, Italian National Institute of Health, Rome; and [3]Department of Endodontics, University 'G. D'Annunzio', Chieti, Italy

Abstract

Grande NM, Plotino G, Pecci R, Bedini R, Malagnino VA, Somma F. Cyclic fatigue resistance and three-dimensional analysis of instruments from two nickel–titanium rotary systems. *International Endodontic Journal*, **39**, 755–763, 2006.

Aim To determine how instrument design affects the fatigue life of two nickel–titanium (Ni–Ti) rotary systems (M*two* and ProTaper) under cyclic fatigue stress in simulated root canals.

Methodology Cyclic fatigue testing of instruments was performed in stainless steel artificial canals with radii of curvature of 2 or 5 mm and an angle of curvature of 60°. A total of 260 instruments were rotated until fracture occurred and the number of cycles to failure were recorded. The morphology of Ni–Ti rotary instruments was investigated by measuring the volume of millimetre slices of each instrument size starting from the tip to the shank by means of μCT analysis. The fracture surface of three representative samples of each size was analysed by scanning electron microscopy (SEM). Data were analysed by one-way ANOVA, Holm *t*-test, paired *t*-test and linear regression; the significance was determined at the 95% confidence level.

Results Cycles to failure significantly decreased as the instrument volume increased for both the radii of curvature tested ($P < 0.01$). The radius of curvature had a statistically significant influence on the fatigue life of the instruments ($P < 0.05$). Larger instruments underwent fracture in less time under cyclic stress than smaller ones. SEM evaluation showed typical features of fracture through fatigue failure.

Conclusions The metal volume in the point of maximum stress during a cyclic fatigue test could affect the fatigue life of Ni–Ti rotary instruments. The larger the metal volume, the lower the fatigue resistance.

Keywords: 3D microcomputerized tomography, 3D volumetric analysis, cyclic fatigue testing, Ni–Ti rotary instruments.

Received 27 October 2005; accepted 6 March 2006

Introduction

The unexpected failure of nickel–titanium (Ni–Ti) rotary instruments inside the root canal during root canal treatment is a matter of serious concern, as these instruments can undergo fracture within their elastic limit without any visible sign of previous permanent deformation (Pruett *et al.* 1997, Sattapan *et al.* 2000).

Fracture of instruments used in rotary motion occurs in two different ways: torsional and flexural or fatigue (Serene *et al.* 1995, Sattapan *et al.* 2000). Fracture because of torsion occurs when the tip or another part of the instrument binds in a canal whilst the shank continues to rotate. When the elastic limit of the metal is exceeded by the torque exerted by the handpiece, fracture of the tip becomes inevitable (Martin *et al.* 2003). Fracture because of flexural fatigue occurs when the instrument does not bind, but rotates freely in a curvature, generating tension/compression cycles at the point of maximum flexure until fracture occurs (Pruett *et al.* 1997, Haikel *et al.* 1999).

Correspondence: Dr Gianluca Plotino, Via Eleonora Duse 22, 00197 Rome, Italy (Tel.: +39068072289; fax: +390688644341; e-mail: gplotino@fastwebnet.it).

Resistance of rotary instruments to cyclic fatigue is affected by the angle and radius of canal curvature and the size and taper of the instrument. Increased severity in the angle and radius of the curves around which the instrument rotates decreases instrument lifespan (Pruett *et al.* 1997, Mize *et al.* 1998, Haikel *et al.* 1999). Instruments have been tested in canals having radii of 2, 5 and 10 mm, with the conclusion that the smaller the radius, the shorter the life of the instrument when rotating (Pruett *et al.* 1997, Haikel *et al.* 1999). Similarly, several studies have shown that increased diameter at the point of maximum curvature of the instrument, which is determined by tip size and taper, reduces the time to fracture (Serene *et al.* 1995, Pruett *et al.* 1997, Haikel *et al.* 1999, Gambarini 2001, Melo *et al.* 2002, Peters & Barbakow 2002). Only the study by Yared *et al.* (2000) did not support these findings. Ruddle (2002) has asserted that the position of the curvature of a canal is a factor in instrument safety, a point that was demonstrated in an earlier study (Malagnino *et al.* 1999). When the curvature is localized in a coronal portion of the root canal, the instrument is subjected to the maximum stress in the area in which its diameter is largest.

Two investigations of the causes of instrument fracture in metal-simulated canals have concluded that rotational speed generally is not a significant factor (Pruett *et al.* 1997, Mize *et al.* 1998). The influence of the morphology of a Ni–Ti rotary file on its performance has been the subject of a number of recent investigations (Turpin *et al.* 2001, Biz & Figueiredo 2004, Diemer & Calas 2004, Chow *et al.* 2005). However, how and why the design of the instrument could influence their behaviour under cyclic fatigue stress remains unclear. Indeed, when instruments of identical size and taper but different design, i.e. Profile, Hero and Quantec, were tested in the same device, the results varied (Haikel *et al.* 1999). Yet, a separate study found that instrument design did not influence the fatigue resistance of instruments of the same size, i.e. ProFile and Quantec (Melo *et al.* 2002).

The aim of the present study was to examine whether instrument design affects the fatigue life of two Ni–Ti rotary systems, M*two* and ProTaper, when subjected to cyclic fatigue stress in simulated root canals.

Materials and methods

Two Ni–Ti endodontic instrument systems were tested: ProTaper (Dentsply Maillefer, Ballaigues, Switzerland) and M*two* (Sweden & Martina, Due Carrare, Italy). The ProTaper system features five instruments: S1, S2, F1, F2 and F3. The SX instrument was not tested because it was designed for a different clinical purpose. The ProTaper instruments have a convex triangular cross-sectional design (Fig. 1a) and combine multiple tapers within the shaft. ProTaper F3 has a reduced cross section in the mid-coronal portion and a U-shaped design to increase its flexibility (Fig. 1b). The M*two* system features seven instruments of varying size and taper: size 10, 0.04 taper; size 15, 0.05 taper; size 20, 0.06 taper; size 25, 0.06 taper; size 30, 0.05 taper; size 35, 0.04 taper; size 40, 0.04 taper). The size 25, 0.07 taper instrument was not tested because it was designed for a different clinical purpose. M*two* instruments have an 'Italic S' cross-sectional design with two blade-cutting surfaces (Fig. 1c).

3D volumetric analysis

One instrument from each size within both instrument systems was analysed three-dimensionally. The morphology of the 12 Ni–Ti rotary instruments tested was

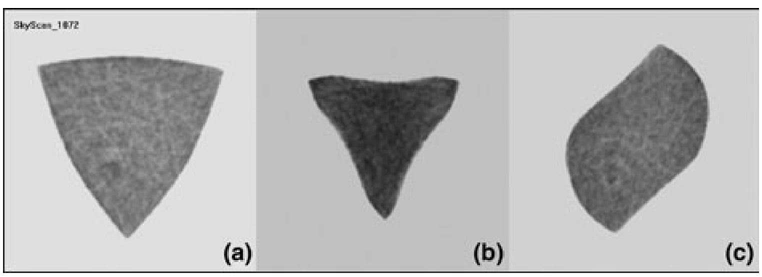

Figure 1 Cross-section obtained by means of μCT scanning and reconstruction of a ProTaper F2 instrument showing the convex triangular design (a), of a ProTaper F3 instrument showing the modified triangular design with deeper flutes (b) and of a M*two* size 25, 0.06 taper instrument showing the two blade cutting surfaces resulting in an 'Italic S' design (c).

investigated by measuring the volume of each millimetre of each instrument, from the tip to the shank. The volume of each millimetre of the apical 10 mm of each instrument was measured (*Vol per mm*). The volume of the millimetre at the point of maximum curvature (between D5 and D6) was recorded, corresponding to the part of the instrument subjected to the maximum stress inside the curvature. This value was recorded as *Vol D5-D6*.

The volumetric analysis was performed using 3D microcomputed tomography (μCT), and the instruments were reconstructed to evaluate the *Vol per mm*.

The scanning procedure was performed in two stages of 4 h each using a desktop X-ray microfocus CT scanner (SkyScan 1072, Aartselaar, Belgium) with a 10 W, 100 kV, 98 μA, a 1.0-mm aluminium filter, and 45 magnification, which resulted in a pixel size of 11.2 × 11.2 μm. During acquisition, hundreds of 2D projections through 180° of rotation were saved in digital form. To obtain the third dimension, the data stored as projections were then transformed into new two-dimensional images (cross sections) with a pixel size of 11.2 × 11.2 μm and a slice thickness of 13.0 μm.

Computer analysis of the recorded data yielded a 2D image of absorption coefficients. A charge-coupled device detector was then used to realize micrometer-sized resolution images and thus led to a minimum time required for examination of the specimens. These data were stored for later use. The float point format of the reconstructed cross-sections was 1024 × 1024 pixels. A typical data collection reconstruction cycle contained shadow image acquisitions from 200 to 400 views with >180° object rotation.

To recreate the complete 3D objects, serial reconstruction of the cross sections was used, which consisted of one acquisition cycle followed by one 'off-line' reconstruction of the complete 3D object at a resolution of 1024 × 1024 pixels for a maximum of 1024 layers.

Cyclic fatigue-testing device

Previous studies using cylindrical metallic tubes to test the cyclic fatigue life of Ni–Ti rotary instruments report that the tubes do not sufficiently constrain the shafts of the smaller instruments (Pruett *et al.* 1997, Mize *et al.* 1998, Yared *et al.* 1999, 2000). Thus, pilot studies were required to develop a test apparatus that would allow all of the instruments to follow the same radius path within the curvature. The pilot study results (Grande *et al.* 2005) suggested that if the artificial canal is not the same shape and size as the instrument, its trajectory would have a reduced curvature during the test and thus would influence the results of the cyclic fatigue test.

The fatigue-testing device manufactured for this study consisted of a main frame to which was connected a mobile plastic support for the handpiece and a stainless steel block with the artificial canals. The dental handpiece was mounted upon a mobile device that allowed for precise and simple placement of each instrument inside the artificial canal, ensuring 3D alignment and positioning of the instruments to the same depth.

Artificial canals were designed to accommodate each instrument in terms of size and taper, thus providing the instrument with a suitable trajectory. To ensure the accuracy of the size of each canal, a copper duplicate of each instrument was milled using a computer numerical control machining bench (Bridgeport VMC 760XP3, Hardinge Machine Tools, Whiteacres, Leicester, UK). Based on the findings of a pilot study, the copper duplicates were enlarged by 0.2 mm to permit free rotation of the instruments whilst generating minimal torque values. The copper duplicates were constructed according to the curvature parameters that were chosen for the study. With these negative molds, the artificial canals were made using a die-sinking electrical-discharge machining process (Agietron Hyperspark 3, AGIE, Losone, Switzerland) in a stainless-steel block. The blocks were hardened through annealing.

The depth of each artificial canal was machined to the maximum diameter of the instrument +0.2 mm, allowing the instrument to rotate freely inside.

Simulated root canals with an angle of curvature of 60° and radii of curvature of 2 and 5 mm were constructed for each instrument. The centre of the curvature was 6 mm from the tip of the instrument, and the curved segment of the canal was approximately 3 mm length for the 2-mm radius and 6-mm length for the 5-mm radius (Fig. 2). Each artificial canal corresponding to the dimensions of each instrument tested was mounted on the stainless-steel block that was connected to the main frame.

The artificial canal was covered with a tempered glass to prevent the instruments from slipping out and to allow for observation of the rotating instrument. To permit air cooling of the instrument during the test, the glass was grooved, and an air compressor was attached to it.

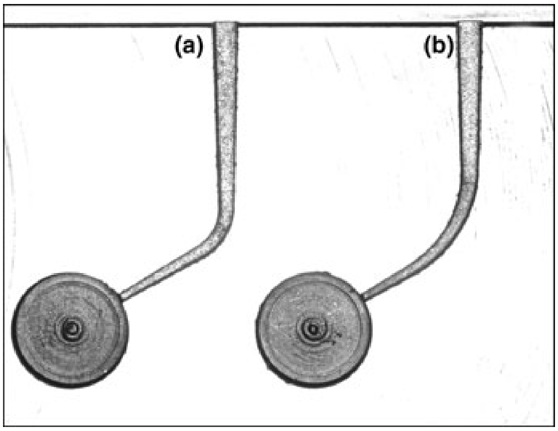

Figure 2 Artificial canals in tempered stainless steel used in the study to test M*two* size 25, 0.06 taper. a: $\alpha = 60°$, $r = 2$ mm; b: $\alpha = 60°$, $r = 5$ mm.

Cyclic fatigue test

Ten instruments of each size from both systems were tested within both two types of artificial canal (240 total). The instruments were rotated at a constant speed of 300 r.p.m. using a 16 : 1 reduction handpiece (W & H Dentalwerk, Burmoos, Austria) powered by a torque-controlled electric motor (Tecnika Digital Torque Control Motor, ATR, Pistoia, Italy). To reduce the friction of the file as it contacted the artificial canal walls, a high-flow synthetic oil designed for lubrication of mechanical parts (Super Oil, Singer, Elizabethport, NJ, USA) was applied.

All instruments were rotated until fracture occurred. The time to fracture for each file was visually recorded with a 1/100-s chronometer, and the number of rotations was calculated to the nearest whole number. The time to fracture was multiplied by the number of rotations per minute to obtain the number of cycles to failure (NCF) for each instrument. Mean values were then calculated. Fracture was easily detectable because the instruments were visible through the glass window.

SEM analysis

Fractured instrument fragments were collected by group. The fracture surface of three representative samples of each size was analysed via scanning electron microscopy (SEM) (Philips SEM 515, Eindhoven, the Netherlands) at 252×, 1550×, and 4020× to determine the characteristics of the fracture process for the test condition.

Statistical analysis

Analysed data consisted of NCF for each instrument tested under the specified radius of curvature, and the volume of the millimetre at the point of maximum curvature of each instrument (*Vol D5-D6*). The data were processed using SPSS software (SPSS, Oakbrook, IL, USA). Means and SD of NCF were calculated for each instrument for both radii of curvature used.

Data were subjected to one-way analysis of variance (ANOVA) to determine significant differences between groups for each radius of curvature tested. When the overall *F*-test indicated a significant difference, the multiple-comparison Holm *t*-test procedure was performed to determine which means differed from the others inside the different radii of curvature. An independent sample *t*-test was used to analyse significant differences between the two radii of curvature for each instrument tested. A multivariate linear regression was performed to investigate the effects of the independent variables considered in the model (i.e. design of the instrument, *Vol D5-D6*, and radius of curvature) on the dependent variable analysed (i.e. NCF).

Results

3D volumetric analysis

The volume of each millimetre (*Vol per mm*) of the apical 10 mm of each instrument is listed in Table 1. Volume values were observed to be related to instrument tip size and taper except in ProTaper F2 and F3. Although the tip size and taper of ProTaper F3 are larger than those of F2, the volume values of F3 were smaller.

Cyclic fatigue test

Means and SDs for the two radii of curvature tested for each instrument, expressed in NCF, are shown in Table 2. The overall regression model was statistically significant ($F = 227.6$; $P = 0.000$; $R^2 = 0.743$). Furthermore, all of the independent variables were statistically significant. The multivariate linear regression showed that the *Vol D5-D6* of the instrument negatively affected the NCF value ($\beta = -3280$), whilst an increase in radius of curvature from 2 to 5 mm positively affected the outcome variable ($\beta = 265$). The M*two* design positively affected the NCF value ($\beta = 151$) when compared with the ProTaper design (Fig. 3).

Table 1 Volume in mm^3 of the first 10 mm of the instruments starting from the tip. The volume between D5 and D6 (*Vol D5-D6*) is in bold

	Mtwo							*ProTaper*				
	10/0.04	15/0.05	20/0.06	25/0.06	30/0.05	35/0.04	40/0.04	S1	S2	F1	F2	F3
Vol D0-D1	0.0041	0.0058	0.0123	0.0216	0.0352	0.0469	0.0599	0.0144	0.0162	0.0234	0.0339	0.0472
Vol D1-D2	0.0101	0.0149	0.0258	0.0399	0.0558	0.0690	0.0853	0.0196	0.0262	0.0426	0.0613	0.0811
Vol D2-D3	0.0179	0.0261	0.0409	0.0607	0.0730	0.0867	0.1033	0.0276	0.0387	0.0634	0.0924	0.1131
Vol D3-D4	0.0278	0.0390	0.0577	0.0822	0.0919	0.1029	0.1221	0.0389	0.0560	0.0836	0.1226	0.1443
Vol D4-D5	0.0387	0.0564	0.0795	0.1103	0.1142	0.1185	0.1399	0.0502	0.0757	0.1073	0.1513	0.1730
Vol D5-D6	**0.0530**	**0.0743**	**0.1035**	**0.1377**	**0.1359**	**0.1398**	**0.1486**	**0.0696**	**0.0996**	**0.1326**	**0.1844**	**0.1841**
Vol D6-D7	0.0668	0.0968	0.1322	0.1725	0.1601	0.1591	0.1690	0.0973	0.1221	0.1584	0.2204	0.2127
Vol D7-D8	0.0841	0.1187	0.1583	0.2070	0.1824	0.1789	0.1944	0.1352	0.1537	0.1844	0.2454	0.2466
Vol D8-D9	0.0999	0.1462	0.1892	0.2365	0.2054	0.1970	0.2205	0.1696	0.1896	0.2237	0.2863	0.2539
Vol D9-D10	0.1194	0.1731	0.2197	0.2716	0.2340	0.2187	0.2474	0.2223	0.2082	0.2463	0.3207	0.3159

Table 2 Mean and SD expressed in number of cycles to failure registered during the cyclic fatigue testing of each instrument for the two radii of curvature tested

	$r = 5$; $\alpha = 60°$		$r = 2$; $\alpha = 60°$	
	Mean	SD	Mean	SD
ProTaper				
S1	303	35	168	41
S2	358	45	139	20
F1	338	51	65	10
F2	72	23	16	3
F3	61	4	12	3
Mtwo				
10/0.04	885	45	465	53
15/0.05	802	143	379	40
20/0.06	644	133	190	35
25/0.06	467	102	72	8
30/0.05	395	15	39	9
35/0.04	381	45	60	18
40/0.04	239	34	20	2

r = radius of curvature.
α = angle of curvature.

The radius of curvature of the canal was found to have a significant effect on NCF for all of the instruments tested. The more abrupt 2-mm radius group had significantly fewer cycles to failure than the 5-mm-radius group for all of the instruments tested ($P < 0.05$ with independent sample *t*-test).

Statistically significant differences were found amongst the different instruments related to their volume and design. The results showed that as *Vol D5-D6* increased, NCF decreased except in ProTaper S1 compared with S2 and in ProTaper S1 compared with F1 for the 5-mm radius and for M*two* size 30, 0.05 taper and size 35, 0.04 taper for the 2-mm radius. However, these differences were not statistically significant ($P > 0.05$ with Holm *t*-test), (Fig. 3).

In the ProTaper group, no statistically significant differences were found amongst S1, S2 and F1 or between F2 and F3 for the 5-mm radius ($P > 0.05$ with Holm *t*-test). For the 2-mm radius, no statistically significant differences were found between S1 and S2 or between F2 and F3 ($P > 0.05$ with Holm *t*-test).

The M*two* instruments tested in the 5-mm radius of curvature showed no statistically significant differences between size 10, 0.04 taper and size 15, 0.05 taper or amongst size 25, 0.06 taper, size 30, 0.05 taper and size 35, 0.04 taper ($P > 0.05$ with Holm *t*-test). For the 2-mm radius, no statistically significant differences were found amongst size 25, 0.06 taper, size 30, 0.05 taper and size 35, 0.04 taper or between size 30, 0.05 taper and size 40, 0.04 taper ($P > 0.05$ with Holm *t*-test).

There were no statistically significant differences amongst ProTaper S1, S2, F1 and M*two* size 30, 0.05 taper and size 35, 0.04 taper or between ProTaper F1 and M*two* size 40, 0.04 taper tested in the 5-mm radius ($P > 0.05$ with Holm *t*-test). For the 2-mm radius, no statistically significant differences were found between ProTaper S1 and M*two* size 20, 0.06 taper, amongst ProTaper F1 and M*two* size 25, 0.06 taper, size 30, 0.05 taper, and size 35, 0.04 taper, or between both ProTaper F2 and F3 and M*two* size 30, 0.05 taper and size 40, 0.04 taper ($P > 0.05$ with Holm *t*-test).

SEM analysis

The fracture surface of instruments of different design and size was similar. The appearance of the fracture surfaces, assessed by SEM, indicated that the breakage of the instruments was the result of fatigue.

The fracture surface revealed a smooth, almost featureless area at the periphery of the fracture face

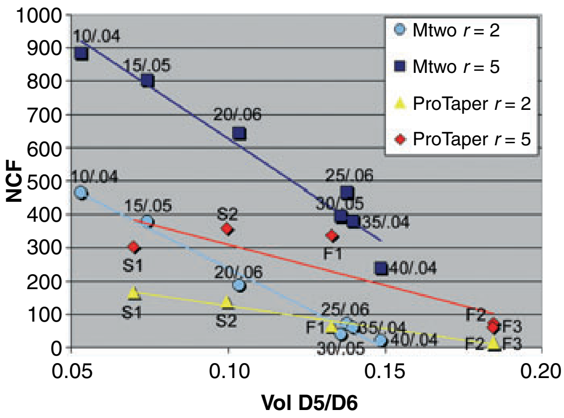

Figure 3 Scatterplot graph of the mean NCF values against *Vol D5/D6*. The slopes of regression lines are quite different for the two brands of instruments, showing that the fatigue resistance is a function of both design and metal mass.

and large central irregular fibrous areas associated with final ductile breakage (Fig. 4a). Areas of crack initiation and growth exhibited small regions of nucleation and slow crack propagation, known as smooth regions, peripheral to the cross section. Crack propagation was typified by striations, each representing the progression of the crack caused by tension during the rotation of the instrument (Fig. 4b). Fractures propagated from the periphery of the instrument towards the centre. Ultimate ductile fracture was observed in the centre of the fracture surface and was characterized by the presence of microvoid crater-like formation and dimpling.

Discussion

Clinically, Ni–Ti rotary instruments are subjected to both torsional load and cyclic fatigue (Gambarini 2001, Yared 2004, Ullmann & Peters 2005), and ongoing research aims to clarify the relative contributions of both factors to instrument separation (Peters 2004).

Both cyclic fatigue tests (Pruett *et al.* 1997, Haikel *et al.* 1999, Fife *et al.* 2004) and torsion tests (Camps & Pertot 1995, Yared 2004, Ullmann & Peters 2005) have been performed to investigate how these factors may influence the behaviour of Ni–Ti rotary instruments *in vitro*. In addition, torsional properties of used instruments have been investigated (Yared *et al.* 2003, Yared 2004, Ullmann & Peters 2005) to analyse how the combination of these two factors may influence instrument failure.

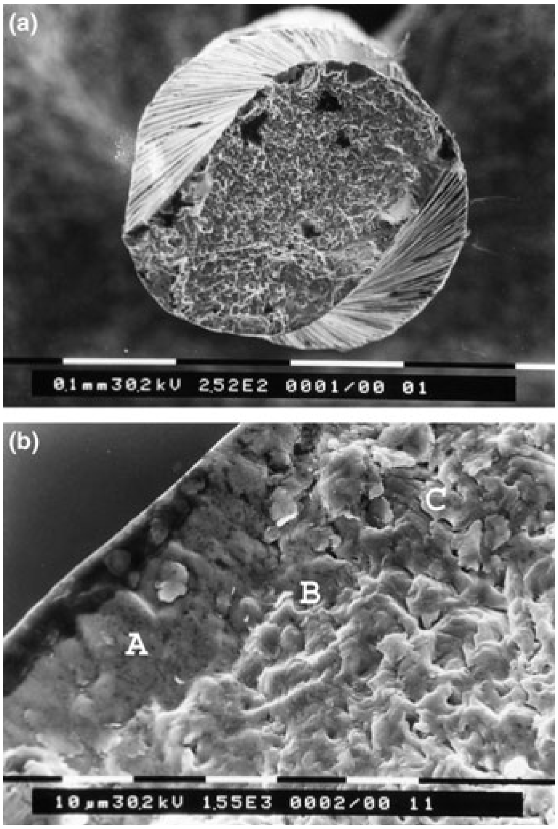

Figure 4 (a) SEM analysis (252×) of the fracture surface of a M*two* instrument after cyclic fatigue testing. It is possible to observe the presence of a smooth, almost featureless area at the periphery of the fracture face and the large central irregular fibrous areas associated with final ductile breakage. (b) Higher magnification of (a) (1550×). Smooth surface at the periphery of the fractured cross-section (A). Areas of crack initiation and growth are characterized by the small areas of nucleation and slow crack propagation, which are called smooth regions (B). Crack propagation was typified by striations (C). Each striation represents the progression of the crack caused by tension during rotation of the instrument.

In the present study, cyclic fatigue resistance tests were performed on two types of Ni–Ti instruments that vary in design and clinical application. The ProTaper instruments have a variable tapered shaft that is designed specifically for a selective crown-down technique, in which successive instruments selectively prepare different areas of the root canal (Clauder & Baumann 2004). The M*two* instruments have constant tapered shaft designed for use in sequence to working length, moving from smaller to larger instruments. The full length of the canal is approached at the same time (i.e. the 'simultaneous technique') (Foschi *et al.* 2004).

In the present study, smaller instruments registered lower *Vol per mm* values. In comparisons of three of the M*two instruments* (size 25, .06 taper, size 30, 0.05 taper, and size 35, 0.04 taper), tip size and taper influenced differently the *Vol per mm*. More specifically, in the apical part of the instrument, tip size had greater influence on the *Vol per mm*, whereas in the coronal part of the instrument, taper had a greater influence on the *Vol per mm*. These instruments have an identical diameter at D5, and the *Vol D5-D6* values for these instruments, not surprisingly, are similar; they decrease coronally along the shaft in the instruments with larger tips and lower tapers.

For the instruments with variable taper, the *Vol per mm* values increased from ProTaper S1 to F3; that is, the *Vol per mm* of S1 was greater than that of S2 in the coronal part of the instrument (D9-D10), because the multiple tapers within the shaft make ProTaper S1 larger than ProTaper S2 at this point. Interestingly, ProTaper F3 showed smaller *Vol per mm* values than F2 between D5 and D10 despite its larger diameter within this part of the instrument. This could be explained by the fact that ProTaper F3 has deeper flutes than the others in the mid-coronal portion (Clauder & Baumann 2004), resulting in a smaller quantity of metal (Fig. 1b). This observation also suggests that the design of the instrument directly influences the *Vol per mm* values. In comparing the design of the two systems, it should be noted that M*two* instruments with a similar tip size registered smaller *Vol per mm* values, although it is difficult to make direct comparisons for the variable taper feature of the ProTaper instruments.

The multivariate linear regression model indicated a significant relationship between the *Vol per mm* and cyclic fatigue resistance. As *Vol D5-D6* increased, NCF decreased except with regard to the ProTaper S1 tested in the 5-mm-radius artificial canal, which registered lower NCF values than ProTaper S2 and F1 (although the differences were not statistically significant). These results concur with those of Fife *et al.* (2004) who showed that ProTaper S1 registered lower NCF than S2, F1 and F2. In the present study, instruments with similar *Vol D5-D6* values have shown similar results. M*two* size 25, 0.06 taper, size 30, 0.05 taper, size 35, 0.04 taper and ProTaper F1 have similar *Vol D5-D6*: 0.137, 0.135, 0.139 and 0.132 mm^3, respectively. No statistically significant differences in NCF were found amongst these instruments for either of the radii of curvature. Moreover, as noted above, ProTaper F3 has a different design (Walsch 2004), resulting in a similar *Vol D5-D6* (0.184 mm^3) to F2. The results obtained in the present study showed no difference in the fatigue life between these two instruments, thus confirming the correlation between metal mass and fatigue resistance.

Conversely, it has been observed that M*two* size 15, 0.05 taper versus ProTaper S1 and M*two* size 20, 0.06 taper versus ProTaper S2 showed different fatigue results despite obtaining similar *Vol D5-D6*. It could be that other factors besides metal mass could influence the fatigue resistance, such as instrument transverse section design. Indeed, the multivariate linear regression model showed a statistically significant association between the design of instrument (analysed as independent variable) and cyclic fatigue resistance. Nevertheless, the regression model could bias the collinear effect between the design analysed variable and *Vol per mm*.

In previous studies, contradictory results regarding the influence of instrument design on fatigue resistance have been reported. Haikel *et al.* (1999) found significant differences in fatigue resistance between different instruments with the same tip diameter and taper tested in the same device, whereas Melo *et al.* (2002) did not.

The *Vol per mm* may be a useful parameter for relating the morphologic characteristics of the instruments to fatigue resistance. This value represents the metal mass of the instrument taking into consideration both the core and the blades, thus being influenced by the different geometric features. It also permits comparisons between nonstandardized instruments in taper and diameter, e.g. ProTaper, for which precise measures along the shaft are difficult to quantify, with standardized instruments, for which taper and diameter are clearly identifiable. For this reason, direct comparison of the influence of cross-sectional design versus *Vol per mm* on the fatigue life of different instruments is needed, using instruments of the same tip and taper and metal volume but different designs.

According to previous studies (Pruett *et al.* 1997, Haikel *et al.* 1999), fatigue life of Ni–Ti rotary instruments is significantly influenced by the radius of curvature. That is, NCF significantly increases as the radius of curvature increases. The multivariate linear regression model has shown that an increase in radius of curvature from 2 to 5 mm positively affects the cyclic fatigue resistance ($\beta = 265$, $P < 0.000$).

In this study, M*two* size 10, 0.04 taper and size 15, 0.05 taper showed the best cyclic fatigue results and a relatively high lifespan under cyclic stress relative to other instruments, and compared to those obtained in similar studies (Haikel *et al.* 1999, Fife *et al.* 2004, Bahia & Buono 2005).

The present study sought to overcome the limitations of some other laboratory studies in terms of the models used for testing. Each artificial canal was specifically designed for each instrument in terms of size and taper, giving it a precise trajectory. Cylindrical metallic tubes used in previous studies (Pruett *et al.* 1997, Mize *et al.* 1998, Yared *et al.* 1999, 2000, Melo *et al.* 2002) did not sufficiently restrict the instrument shaft, which would tend to regain its original straight shape, aligning into a trajectory of greater radius and reduced angle (Yared *et al.* 1999, 2000, Melo *et al.* 2002, Bahia & Buono 2005). If the artificial canal is not identical (in shape and size) to the instrument, its trajectory will not respond to the established parameters, thus having a reduced curvature during the test. This can influence the results of the cyclic fatigue test (Grande *et al.* 2005).

The SDs registered in this study are relatively large considering that the instruments we analysed were new files obtained from the manufacturers. These variations may reflect variability in the manufacturing process rather than in the test procedure, given the standardization of the device used in this study.

Simulated root canals with an angle of curvature of 60° and a radius of curvature of 2 and 5 mm were used based on the findings of Pruett *et al.* (1997) that the stress levels induced by curvatures smaller than 5 mm in radius and 30° in angle did not result in instrument separation within the time frame of their study (5 min).

The point of maximum instrument deformation in fatigue tests is localized to the middle of the curvature (Bahia & Buono 2005), corresponding in the device used in this study to a distance of 6 mm from the tip of the instrument. This is the point most widely used in previous cyclic fatigue studies (Pruett *et al.* 1997, Mize *et al.* 1998, Haikel *et al.* 1999).

Conclusions

The metal mass at the point of maximum stress influenced the lifespan of Ni–Ti rotary instruments during a cyclic fatigue test. The bigger the metal mass, the lower the fatigue resistance. Clinically, this implies that instruments with a greater metal mass should be discarded sooner than smaller instruments.

Instrument metal mass measured as *Vol per mm* by means of μCT analysis appears to be a useful parameter for investigating the mechanical properties of Ni–Ti rotary instruments related to their morphology. Further investigations are required to evaluate the design of other instruments in terms of metal mass and how this parameter could influence the torsional behaviour of Ni–Ti rotary instruments.

Acknowledgements

The authors wish to express their gratitude to Prof. Elisabetta Cotti, Dr Lisa Bywaters, and Dr Josè Luis Marcos Arenal for their help in the preparation of this manuscript. The authors are grateful to Massimo Mariani and P.M.T. for their help in the manufacture of the device used in this study.

References

Bahia MGA, Buono VTL (2005) Decrease in the fatigue resistance of nickel-titanium rotary instruments after clinical use in curved root canals. *Oral Surgery Oral Medicine, Oral Pathology, Oral Radiology and Endodontology* **100**, 249–55.

Biz MT, Figueiredo JAP (2004) Morphometric analysis of shank-to-flute ratio in rotary nickel–titanium files. *International Endodontic Journal* **37**, 353–8.

Camps JJ, Pertot WJ (1995) Torsional and stiffness properties of nickel-titanium K files. *International Endodontic Journal* **28**, 239–43.

Chow DY, Stover SE, Bahcall JK, Jaunberzins A, Toth JM (2005) An in vitro comparison of the rake angles between K3 and Profile endodontic file systems. *Journal of Endodontics* **31**, 180–2.

Clauder T, Baumann MA (2004) ProTaper NT system. *Dental Clinics of North America* **48**, 87–111.

Diemer F, Calas P (2004) Effect of pitch length on the behaviour of rotary triple helix root canal instruments. *Journal of Endodontics* **30**, 716–8.

Fife D, Gambarini G, Britto LR (2004) Cyclic fatigue testing of ProTaper NiTi rotary instruments after clinical use. *Oral Surgery Oral Medicine Oral Pathology Oral Radiology and Endodontology* **97**:251–6.

Foschi F, Nucci C, Montebugnoli L et al. (2004) SEM evaluation of canal wall dentine following use of Mtwo and ProTaper NiTi rotary instruments. *International Endodontic Journal* **37**, 832–9.

Gambarini G (2001) Cyclic fatigue of ProFile rotary instruments after prolonged clinical use. *International Endodontic Journal* **34**, 386–9.

Grande NM, Plotino G, Falanga A, Somma F (2005) A new device for cyclic fatigue testing of NiTi rotary endodontic instruments (Abstract R60). *International Endodontic Journal* **38**, 936–7.

Haikel Y, Serfaty R, Bateman G, Senger B, Allemann C (1999) Dynamic and cyclic fatigue of engine-driven rotary nickel titanium endodontic instruments. *Journal of Endodontics* **25**, 434–40.

Malagnino VA, Passariello P, Corsaro S (1999) The influence of root canal trajectory on the risk of cyclic fatigue failure on Ni-Ti engine driven endodontic instruments. *Giornale Italiano di Endodonzia* **13**, 190–200.

Martin B, Zelada G, Varela P et al. (2003) Factors influencing the fracture of nickel titanium rotary instruments. *International Endodontic Journal* **36**, 262–6.

Melo MCC, Bahia MGA, Buono VTL (2002) Fatigue resistance of engine-driven rotary nickel-titanium endodontic instruments. *Journal of Endodontics* **28**, 765–9.

Mize SB, Clement DJ, Pruett JP, Carnes DL (1998) Effect of sterilization on cyclic fatigue of rotary nickel-titanium endodontic instruments. *Journal of Endodontics* **24**, 843–7.

Peters OA (2004) Current challenges and concepts in the preparation of root canal systems: a review. *Journal of Endodontics* **30**, 559–65.

Peters OA, Barbakow F (2002) Dynamic torque and apical forces of ProFile .04 rotary instruments during preparation of curved canals. *International Endodontic Journal* **35**, 379–89.

Pruett JP, Clement DJ, Carnes DL (1997) Cyclic fatigue of nickel-titanium endodontic systems. *Journal of Endodontics* **23**, 77–85.

Ruddle CJ (2002) Cleaning and shaping the root canal system. In: Cohen S, Burns RC, eds. *Pathways of the pulp*, 8th edn. St Louis: Mosby, pp. 231–92.

Sattapan B, Nervo G, Palamara J, Messer H (2000) Defects in nickel titanium endodontic rotary files after clinical usage. *Journal of Endodontics* **26**, 161–5.

Serene TP, Adams JD, Saxena A (1995) *Nickel-titanium instruments: applications in endodontics*. St Louis, MO, USA: Ishiyaku EuroAmerica.

Turpin YL, Chagneau F, Bartier O, Cathelineau G, Vulcain JN (2001) Impact of torsional and bending inertia on root canal instruments. *Journal of Endodontics* **27**, 333–6.

Ullmann CJ, Peters OA (2005) Effect of cyclic fatigue on static fracture loads in ProTaper nickl-titanium rotary instruments. *Journal of Endodontics* **31**, 183–6.

Walsch H (2004) The hybrid concept of nickel-titanium rotary instrumentation. *Dental Clinics of North America* **48**, 183–202.

Yared GM (2004) In vitro study of the torsional properties of new and used profile nickel titanium rotary files. *Journal of Endodontics* **30**, 410–2.

Yared GM, Bou Dagher FE, Machtou P (1999) Cyclic fatigue of Profile rotary instruments after simulated clinical use. *International Endodontic Journal* **32**, 115–9.

Yared GM, Bou Dagher FE, Machtou P (2000) Cyclic fatigue of Profile rotary instruments after clinical use. *International Endodontic Journal* **33**, 204–7.

Yared G, Kulkarni GK, Ghossayn F (2003) Torsional properties of new and used rotary K3 NiTi files. *Australian Endodontic Journal* **29**, 75–8.